

A HYBRID PNEUMATIC/ELECTROSTATIC MILLI-ACTUATOR*

Kenneth H. Chiang, Ronald S. Fearing†

Robotics and Intelligent Machines Laboratory

Department of Electrical Engineering and Computer Sciences

265M Cory Hall

University of California, Berkeley, CA 94720-1770

ronf@eecs.berkeley.edu

ABSTRACT

In typical MEMS applications, actuation is accomplished directly by converting electrical input power to useful mechanical power. However, indirect schemes employing electrically driven primary and alternately driven secondary actuators can trade simplicity and bandwidth for lower forces and strokes in the primary actuator, hence reducing power consumption.

Because it is generally easier to build actuators with high force and low stroke, we propose a hybrid actuator with a pneumatic oscillator as the secondary and an electrostatic clamp as the primary. By clamping the oscillator at its extremes of travel, the hybrid actuator can be turned on and off.

In this paper, we report on progress towards fabricating such a hybrid actuator. We have demonstrated operation of a $40 \times 40 \times 30 \text{ mm}^3$ oscillator at 6 Hz with a stroke of 2.5 mm and a peak force of 1.1 N, although fabrication of the electrostatic clamp has not been accomplished.

INTRODUCTION

In typical MEMS applications, actuation is accomplished directly by converting electrical input power to useful mechanical power. Direct actuation is simpler, but many tasks require higher forces and strokes. On the other hand, using a set of primary and secondary actuators trades simplicity and bandwidth for lower forces and strokes in the primary actuator. Moreover, if there is power available from other non-electrical sources and bandwidth to spare, the secondary actuator can be driven with the alternative power source, providing power gain for the electrically-driven primary actuator.

Consider an actuator, such as one for a tactile display [Moy, 2000], which requires a pressure of 5 atm, a stroke of 1.5 mm, a bandwidth of 100 Hz, and a packaged volume of 40 mm^3 ; that is, a power density of 7.5 W/cm^3 . No current MEMS actuators can meet these specifications [Fearing, 1998], but they are easily met by

pneumatics. 5 atm of air acting across a 1 mm^2 membrane exerts a force of 0.5 N, and if that membrane is made of sufficiently thin silicone rubber, it can deflect more than 0.5 mm before bursting. In addition, 18 mm^3 volumes can be charged to 5 atm gage in 0.5 ms through a 0.5 mm diameter orifice, and discharged in less than twice that time.

Additionally, a brief survey of the available valve literature, as shown in Figure 1, reveals that there are no commercially available valves that satisfy the size and power density requirements for the tactile display.

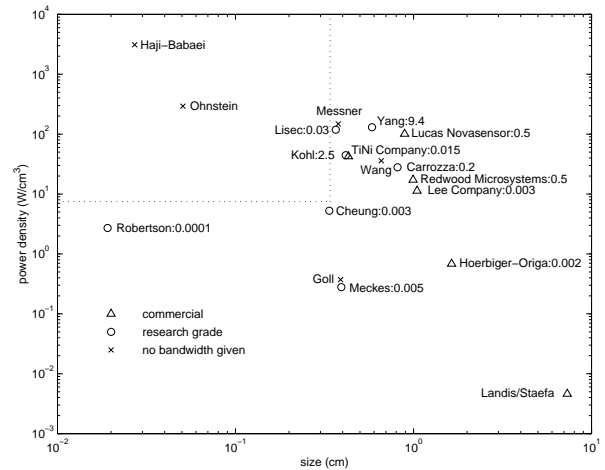


Figure 1: Representative valve designs [Cheung, 1997, Carrozza, 1996, Goll, 1997, Haji-Babaei, 1997, Kohl, 1999, Lisee, 1996, Meckes, 1997, Messner, 1998, Ohnstein, 1990, Robertson, 1996, Yang, 1997, Hoerbigier-Origa, Landis/Staefa, Lee Company, Lucas Novasensor, Redwood Microsystems, TiNi Alloy, Wang, 2000]. Designs are labeled with author or company name, and actuation time in seconds. Any designs in the upper left corner with actuation times less than 10 ms satisfy the power density and size requirements for the tactile display of [Moy, 2000].

*This work was funded in part by NSF grant IRI-9531837.

†Address all correspondence to this author.

For valves without force balancing, for an orifice of

0.5 mm diameter and a pressure difference of 5 atm, a worst-case force of 100 mN needs to be generated over a stroke of 0.125 mm to operate a poppet that can drive such a pneumatic actuator. Thus, the pneumatic valve requires significant mechanical power for its drive. As argued above, indirect drive is preferable to direct drive, and we also have an alternate power source available—the compressed air itself. A piloted servovalve is usual practice in such situations; the output of a small primary valve is amplified by the larger secondary servovalve. Unfortunately, we still need an actuator for the pilot valve, although the force and stroke are reduced.

We note that it is generally easier to build electric actuators with high force and small stroke than the converse. Thus, we propose a hybrid actuator with a pneumatic oscillator as the secondary actuator and an electrostatic clamp as the primary actuator. By clamping the oscillator at the extremes of its motion, the hybrid actuator can be turned on and off.

In our design, the pneumatic oscillator has a membrane that moves back and forth as the pressure difference across the membrane changes. As the membrane moves to one side, a magnet embedded in the membrane triggers a magnetically-actuated valve to switch open. Because of positive feedback, opening the valve alters the pressure difference across the membrane, forcing it back. The magnet then moves away from the valve, closing it again. The pressure difference falls again as air discharges through an orifice, and the membrane moves towards the valve again, repeating the cycle.

By clamping the membrane at either end of its range of travel, the oscillator can be stopped. This clamping can be accomplished by an electrostatic actuator. By energizing the clamp at the appropriate time, the oscillation frequency can be modulated. Because the membrane is moved by the oscillator and not the electrostatic primary actuator, the primary only needs to clamp and hold the membrane.

For the 10:1 scale prototype that was constructed, at 5 Hz, such a primary actuator consumes a theoretical 0.22 mW. For comparison, consider the Hoerbiger-Origa Piezo 2000, a commercially available directly-driven valve, that consumes 0.14 mW at the same frequency, at an operating pressure of 2.2 atm absolute with nominal flow rate of 25 ml/s[Hoerbiger-Origa]. It is expected that an at-scale prototype would have a lower power consumption.

In this paper, we report on progress towards fabricating such a hybrid actuator, intended to operate at 100 Hz with a stroke of 0.5 mm and a peak force of 100 mN. We have demonstrated operation of a 40x40x30 mm³ oscillator at 5–6 Hz with a stroke of 2.5 mm and a peak force of 1.1 N.

OSCILLATOR, THEORETICAL BASIS

We begin with an electrical analogue to a pneumatic oscillator, as shown in Figure 2. The operational amplifier and three lower resistors form a Schmitt trigger. With the addition of a resistor and capacitor combination connecting the

output voltage to the inverting terminal, a self-starting electrical oscillator is formed. The oscillation frequency is controlled by the time constant of the resistor-capacitor combination, as well as the switching voltages of the Schmitt trigger positive feedback, and the supply voltage.

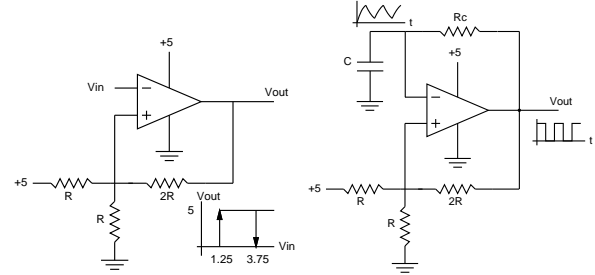


Figure 2: An electrical analogue to a pneumatic oscillator. The Schmitt trigger at left switches at 1.25 V and 3.75 V. Adding a resistor and capacitor gives the electrical oscillator at right. The waveforms for V_{out} and the voltage across capacitor C are also sketched.

The key elements of the electrical oscillator are the Schmitt trigger with its hysteretic relay characteristic, and the capacitor with its integrating action. A pneumatic oscillator should then have both of these elements, with mechanical feedback between the pressure in the accumulator and whatever serves as the relay.

A pressure-actuated normally closed diaphragm valve could realize that relay characteristic, with the appropriate diaphragm design prestressed so that it opens above a certain pressure and closes below a lower pressure. However, it was felt that critical elements should be material-independent and repeatedly realizable.

Fortunately, there are other ways to provide the desired characteristic; for instance, a single-ended pneumatic cylinder whose rod is mechanically attached to a normally closed valve forms a pressure actuated valve. Hysteresis can then be added by putting detents on the rod with the right spring loading, so that the rod stays in one of two positions. This is illustrated in Figure 3. If the piston has cross sectional area

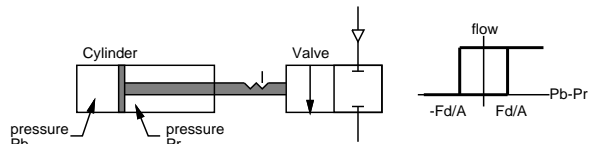


Figure 3: A pneumatic relay with hysteresis can be constructed from a single-ended pneumatic cylinder and two-position normally-closed valve (left). The valve is mechanically connected to the cylinder, and the detents on the rod result in the hysteretic relay transfer function between the pressure difference across the cylinder piston and the flow through the valve (right).

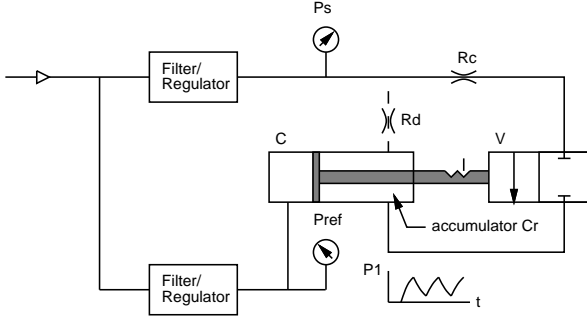


Figure 4: Pneumatic oscillator. The rod side of single-ended cylinder C is an accumulator C_r whose pressure alternately rises and falls as the rod travels back and forth, opening and closing valve V to charge C_r through restriction R_c . C_r discharges through R_d . The detents on the rod provide hysteresis.

A and the force required to move between the detents is F_d , when $P_b - P_r$ is greater than F_d/A , the valve should open, assuming the rod occupies negligible area on the face of the piston. When the pressure difference is less than $-F_d/A$, the valve should close. This gives the desired hysteretic relay transfer function.

With the appropriate connections, the relay above can then be turned into an oscillator. First, the valve inlet is connected to the air supply, and the valve outlet to the rod side of the cylinder, where flow through the valve charges the cylinder, closing the valve when the cylinder pressure reaches a critical value. Second, the blind side of the cylinder is connected a pressure reference that ensures the valve will tend to be opened; this is analogous to the voltage divider in the Schmitt trigger of Figure 2. Finally, orifices are added to discharge the cylinder rod side and limit the charging rate through the valve. The resulting pneumatic circuit is shown in Figure 4.

OSCILLATOR, IMPLEMENTATION

A realization of the pneumatic circuit of Figure 4 is in Figure 5. To eliminate leakage between the rod and blind sides of cylinder, as well as reduce friction effects, a moving membrane is substituted for the moving piston. Hysteresis is provided by embedding a permanent magnet in this membrane, and placing two steel pieces at each end of the cylinder, instead of using detents. To eliminate leakage from the cylinder, the mechanical connection between the valve and cylinder is replaced with a magnetic one. The valve is made magnetically actuated by fabricating the poppet out of steel; this is the leftmost of the steel pieces shown. Note that the chamber formed by the membrane and the valve body, to which the reference pressure source is connected, is referred to as the reference chamber, and that the chamber to which the magnetically-actuated valve is attached is referred to as the working chamber.

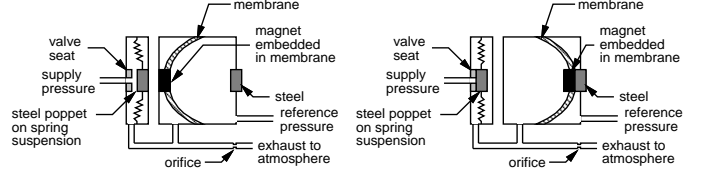


Figure 5: A realization of the pneumatic oscillator shown schematically in Figure 4, showing the oscillator at both extremes of motion, with magnetically-actuated valve open at left, and the same valve closed at right.

A more detailed description of the operation of the oscillator is given in the next section.

OSCILLATOR, SIMULATION AND ANALYSIS

There are a number of equations that govern the resulting system:

- the deflection of the membrane due to the pressure difference across the membrane,
- the force from the magnet on the membrane,
- the mass flow rate through the magnetically-actuated valve,
- the mass flow rate through the discharge orifice,
- and the variable volume cylinder formed by the oscillator body and the membrane.

Assuming that the membrane moves slowly enough so that quasi-static approximations apply, the forces on the membrane determine the position of the membrane, which in turn determines the opening or closing of the magnetically-actuated valve. As the pressure difference across the membrane changes with the opening and closing of the valve, the balance of forces changes, closing the loop and causing the system to oscillate.

From [Timoshenko, 1959, p. 69], the deflection w of the membrane center due to a point load P is:

$$w = \frac{Pa^2}{16\pi D} \quad (1)$$

where a is the membrane radius, and $D = \frac{Eh^3}{12(1-\nu^2)}$, with E being the membrane modulus, ν Poisson's ratio for the membrane, and h the membrane thickness. From [Hermida, 1998], the deflection w of the membrane center due to a pressure difference q across the membrane is:

$$w = \alpha a^3 \sqrt{\frac{qa}{Eh}} \quad (2)$$

where $\alpha = 0.278$ for material with Poisson's ratio of 0.5, a is the membrane radius, E is the membrane modulus, and h is the membrane thickness. Assuming superposition applies, the total deflection of the membrane center is the sum of these two quantities.

The force on the membrane is approximated as a point load from the embedded cylindrical magnet on the

steel pieces at either end of the cylinder. Following [Magnet Sales and Manufacturing] to determine this point load, the flux density $B(x)$ at a distance x away from the surface of a cylindrical magnet with radius R and length L is:

$$B(x) = \frac{B_r}{2} \left(\frac{L+x}{\sqrt{R^2 + (L+x)^2}} - \frac{x}{\sqrt{R^2 + x^2}} \right) \quad (3)$$

where B_r is the residual flux density of the magnet and the distance is measured along the centerline of the magnet. In this case, the cylindrical magnet lies between two steel pieces. Assuming that the steel pieces are perfect ferromagnetic half-planes, if they are a distance d apart, then one face of the magnet lies a distance x away from one steel piece and a distance $d - L - x$ away from the other. The flux density is then $2B(x)$ and $2B(d - L - x)$, respectively, and the total force on the magnet is approximately:

$$F = \frac{4B(x)^2 - 4B(d - L - x)^2}{2\mu_0} A \quad (4)$$

where μ_0 is the magnetic permeability and A the cross-sectional area of the magnet. A plot of this force is given in the bottom half of Figure 7.

Referring to Figure 5, when the membrane has moved completely to the left, the embedded magnet opens the magnetically-actuated valve. The resulting pneumatic model is of an orifice charging a variable volume cylinder, with another orifice discharging that cylinder. When the membrane has moved completely to the right, the magnetically-actuated valve is closed, and the resulting pneumatic model is solely of the discharge orifice emptying the cylinder. The magnetically-actuated valve is modeled as either open or closed, open being defined as membrane within a small distance of the leftmost travel of the membrane, and closed being greater than this threshold.

Both the open magnetically-actuated valve and the discharge orifice are modeled following [Blackburn, 1960], where the mass flow rate \dot{m} through an orifice is given by:

$$\dot{m} = \begin{cases} C_c A_0 \sqrt{P_1 \rho_1^{\frac{2k}{k-1}} \sqrt{\left(\frac{P_2}{P_1}\right)^{\frac{2}{k}} - \left(\frac{P_2}{P_1}\right)^{\frac{k+1}{k}}} \text{ if } \frac{P_2}{P_1} \leq 0.528} \\ C_c A_0 \sqrt{P_1 \rho_1^{\frac{2k}{k-1}} \sqrt{(0.528)^{\frac{2}{k}} - \left(\frac{P_2}{P_1}\right)^{\frac{k+1}{k}}} \text{ otherwise} \end{cases} \quad (5)$$

where C_c is the contraction coefficient, A_0 is the effective cross-sectional area of the orifice, P_1 is the upstream pressure, ρ_1 is the upstream density, P_2 is the downstream pressure, and k is the ratio of specific heats.

Under quasi-static assumptions, for the variable volume cylinder formed by the oscillator body and the membrane, the relationship between the change in pressure \dot{P} and the mass flow rate \dot{m} is:

$$\dot{P} = \frac{nRT}{V} \dot{m} \quad (6)$$

where n is the process constant, R the gas constant, T the gas temperature, and V the cylinder volume. The process is

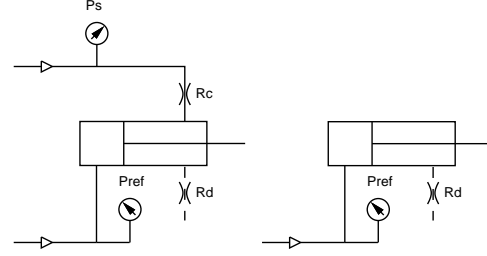


Figure 6: Pneumatic models of the oscillator with the magnetically-actuated valve open (left) and with the magnetically-actuated valve closed (right), corresponding to the left and right of Figure 5, respectively.

assumed to be adiabatic, following [Shearer, 1956], so $n = k$, the ratio of specific heats as above.

Pneumatic models corresponding to the cases where the magnetically-actuated valve are open and closed are shown in Figure 6.

A simulation was constructed using these equations, with relevant parameters given in Table 1. A representative trajectory is plotted in the upper half of Figure 7. With the membrane at its leftmost position of travel, the magnet embedded in the membrane holds the magnetically-actuated valve open, as shown in the left of Figure 5. The pressure in the working chamber begins at atmospheric pressure, and increases until the pressure difference across the membrane is great enough to overcome the attractive force between the embedded magnet and the valve, whereupon the membrane snaps to the right. As noted previously, this provides the desired hysteresis. With the membrane at its rightmost position, the valve closes and the working chamber pressure falls until the pressure difference is great enough to overcome the attractive force between the embedded magnet and the steel piece in the reference chamber, as shown at the right of Figure 5. The membrane then snaps to the left, and the cycle repeats. Note from the times indicated on the state trajectory that the snapping action happens relatively quickly compared to the charging and discharging times of the working chamber.

In an analogy to the electrical oscillator mentioned previously:

- once the membrane has crossed the center position, the magnet force provides the snap action that corresponds to the high gain of the desired hysteretic relation,
- while the membrane is at its extremes of travel, the membrane modulus and thickness, together with the magnet force, determine the pressures at which the membrane switches position,
- and the volume of the working chamber, the diameters of the magnetically-actuated valve and the discharge orifice, and the supply and exhaust pressures set the switching frequency.

parameter	symbol	10:1 prototype	proposed 1:1
supply pressure	P_s	1.9 atm abs	2.0 atm abs
reference pressure	P_{ref}	1.25 atm abs	1.25 atm abs
exhaust pressure	P_{ex}	1 atm abs	1 atm abs
gas temperature	T	293 K	293 K
ratio of specific heats	k	1.4	1.4
valve diameter	D_c	0.66 mm	0.5 mm
discharge orifice diameter	D_d	0.41 mm	0.2 mm
contraction coefficient	C_c	0.6	0.6
valve switching threshold		0.25 mm	0.1 mm
cylinder diameter	D_{cyl}	24 mm	3 mm
cylinder initial volume	V_0	4500 mm ³	20 mm ³
membrane modulus	E_{mem}	400 kPa	400 kPa
membrane Poisson ratio	ν_{mem}	0.5	0.5
membrane radius	a_{mem}	12 mm	1.5 mm
membrane thickness	h_{mem}	2 mm	0.5 mm
membrane travel	x_{mem}	0 – 2.5 mm	0 – 0.5 mm
magnet radius	R_{mag}	2.38 mm	0.75 mm
magnet length	L_{mag}	7.94 mm	1 mm
residual flux density	B_r	0.575 T	0.64 T
magnet separation	L	13.44 mm	2.3 mm
magnet travel	x_{mag}	1.5 – 4.0 mm	0.4 – 0.9 mm
oscillation frequency	f	10 Hz	350 Hz
dielectric thickness	d_{es}	3 μ m	2.5 μ m
relative permittivity	ϵ	2	2
applied voltage	V_{es}	180 V	180 V
clamp pressure	P_{es}	32 kPa	46 kPa
clamp capacitance	C_{es}	2.7 nF	50 pF
theoretical power consumption for electrostatic clamp	P	0.22 mW at 5 Hz	81 μ W at 100 Hz

TABLE 1: Simulation parameters for 10:1 scale prototype and proposed at-scale device.

Simulation results, with parameters set according to Table 1, have been compared to actual results from a 10:1 scale prototype of this oscillator, shown in Figure 8. The prototype, with the supply and reference pressures set appropriately and with the correct discharge orifice attached to the entire system, has been observed to oscillate without failure at 5 – 6 Hz for approximately 15000 cycles, a portion of which is shown in Figure 9. Comparing Figure 10 with Figure 9, the simulation oscillates at approximately twice the frequency actually observed in the prototype, which is within reasonable limits.

Possible sources of error include:

- the membrane model may not be applicable for large strain conditions,
- the shape of the membrane forming one side of the variable volume cylinder is modeled as a cone,
- the magnet parameters are unverified, due to lack of a gaussmeter,
- the pressure losses through lines are unmodeled,
- the reference pressure is modeled as constant,
- and the magnetically actuated valve is modeled as being either open or closed.

Oscillation in the simulation was not observed except for certain critical parameter values, indicating that the simu-

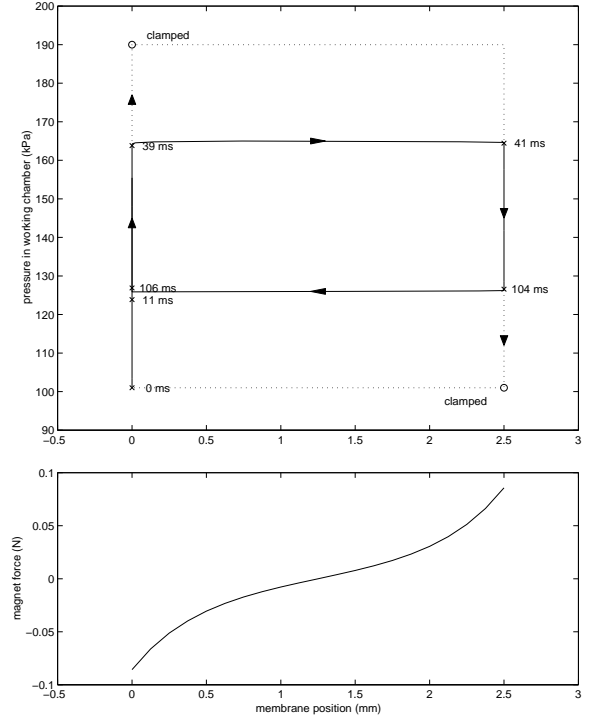


Figure 7: Simulated state trajectory (solid line in upper plot), relating membrane position and pressure in the working chamber, with force on membrane due to magnetic attraction between the embedded magnet and steel endpieces plotted below. When the membrane is clamped at either end of its travel, the system follows the dotted trajectory, and stops at the circled points in state space; when released, the system continues to follow the dotted trajectory until it rejoins the solid state trajectory. A position of 0 mm corresponds to the situation illustrated in the left of Figure 5, and a position of 2.5 mm corresponds to that illustrated in the same figure at the right.

lation is very sensitive to those parameters. Another major problem is that the peak magnet force was measured to be 1.1 N, as opposed to the 85 mN of the simulation. This discrepancy is most likely due to the assumptions made in the modeling of the membrane.

ELECTROSTATIC CLAMP

Although the electrostatic clamp[Monkman, 1988] is as yet unfabricated, simulation results indicate that the oscillator prototype can be held at either end of its travel by a potential difference V of 180 V applied across a dielectric with a permittivity ϵ of 2, with a thickness d of 3 μ m. With this potential applied, the clamp exerts an equivalent pressure of $P_{es} = \frac{1}{2}\epsilon\epsilon_0(\frac{V}{d})^2$, or 32 kPa.

The clamping works because the equivalent pressure of the clamp adds to the pressure difference across the mem-

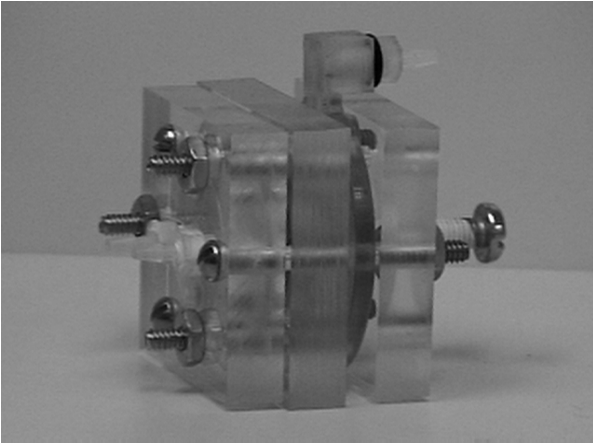


Figure 8: 10:1 scale prototype of the pneumatic oscillator, with dimensions $40 \times 40 \times 30 \text{ mm}^3$.

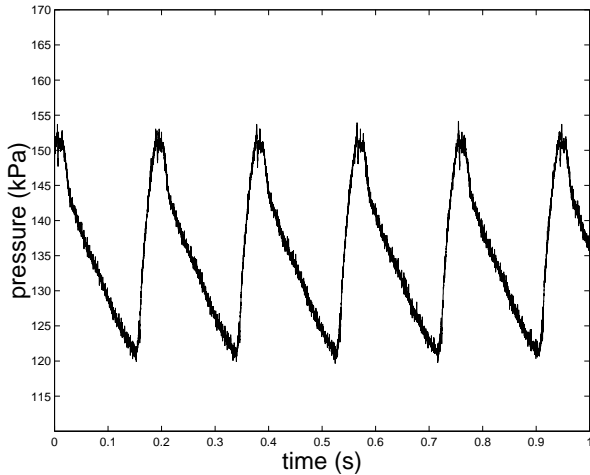


Figure 9: Pressure in the working chamber as a function of time for the 10:1 scale prototype of the pneumatic oscillator. The frequency of oscillation is thus correspondingly lower than the intended 100 Hz, because the cylinder volume is 500 times larger. The waveform is also asymmetric because the charge and discharge orifices have different diameters.

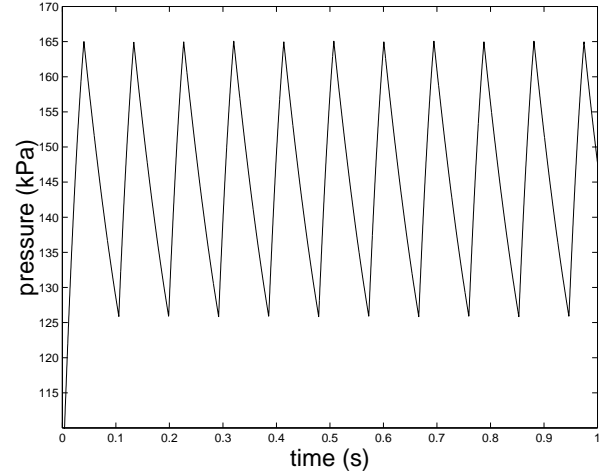


Figure 10: Pressure in the working chamber as a function of time for the simulation of a 10:1 scale prototype of the pneumatic oscillator. The oscillation frequency is twice that of the actual prototype, for reasons noted in the text.

brane. Consult Figure 7 and consider the case when the membrane is at 0 mm, and the working chamber pressure is at 125 kPa; if the clamp is applied then, the pressure in the working chamber, which ordinarily would rise to 165 kPa, would need to rise to 197 kPa before the membrane would snap away from the magnet and move to the 2.5 mm position. However, because the supply pressure is set to 190 kPa, that critical pressure would not be reached, effectively clamping the membrane at 0 mm. A similar argument can be made for the 2.5 mm position; with the clamp applied, the working chamber pressure would need to fall below $125 - 32$, or 93 kPa, but the exhaust pressure is set to 101 kPa.

Such an electrostatic clamp could be constructed by making the membrane out of a conducting material, and using the valve body as the other electrode. The valve body could be coated with a thin layer of dielectric material, and the potential difference applied across the membrane and body. For the 10:1 scale prototype switching at $f = 5 \text{ Hz}$, the capacitance is $C_{es} = \frac{\epsilon\epsilon_0 A}{d}$, or 2.7 nF, and the power consumed is $P = \frac{1}{2} C_{es} V^2 f$, or 0.22 mW.

HYBRID ACTUATOR, MILLISCALE

Simulations were also performed with parameter values set for an at-scale prototype of the hybrid actuator, as given in Table 1. In all other respects, the model was the same as that for the 10:1 scale prototype, including a quasi-static membrane model. An oscillation frequency of approximately 350 Hz was predicted from the simulation results, although whether the quasi-static assumption can be said to hold is questionable. In addition, because the peak magnet force from the actual 10:1 scale prototype was an order of magnitude off from that of the simulation, extrapolation of

the model to at-scale dimensions is also suspect.

However, the electrical oscillator, upon which the pneumatic oscillator is based, is in general robust to parameter variations, provided the gain of the Schmitt trigger is high enough. By appropriate membrane design and choice of magnet parameters, high gain can be achieved.

CONCLUSIONS/FUTURE WORK

Initial investigation of the oscillator and simulation seem encouraging, but the electrostatic clamp has not been implemented. Theoretical calculations for the clamp indicate the potential of the idea of driving a secondary actuator with an alternate power source and braking that secondary with an electrically-driven primary actuator, but the true test will come in the implementing and demonstrating a complete prototype that has both oscillator and clamp. Constructing the electrostatic clamp may be prove to be difficult, because of the thin coating and high field strength that would be required.

For an at-scale prototype, in addition to the clamp being a problem, embedding small magnets in the membrane that are sufficiently strong to provide hysteresis may also prove to be problematic.

Application of the hybrid actuator is more straightforward. The oscillating pressure in the working chamber can be tapped to drive another actuator, as long as it does not heavily load the oscillator. Perhaps an even simpler method might be to replace the steel piece in the reference chamber with another magnetically-actuated valve, which can then be driven in a pulse-width modulated fashion. If such a valve were to be attached, metering a 2 atm absolute pressure at a flow rate of 25 ml/s, the resulting milli-actuator potentially would have a power gain of 2100 from electrical to mechanical power at an operation frequency of 100 Hz.

Overall, initial results will need to be expanded upon before a definitive statement about this idea can be made. However, the design has a large number of degrees of freedom, specifically in the choice of magnet and membrane parameters. More generally, other mechanisms with hysteresis may be employed, and certainly there is much room for further optimization.

ACKNOWLEDGEMENTS

The authors would like to thank S Avadhanula, G Moy, E Shimada, H Shinoda, U Singh, M Sitti, J Thompson, C Wagner, R Wood, J Yan, and W Zesch for their insights and otherwise helpful discussions.

REFERENCES

- [Blackburn, 1960] JF Blackburn, G Reethof, JL Shearer, *Fluid Power Control*, Cambridge: MIT Press, 1960.
- [Carrozza, 1996] MC Carrozza, L Lencioni, B Magnani, P Dario, D Reynaerts, MG Trivella, A Pietrabissa, "A microrobot for colonoscopy," *MHS'96 Proceedings of the Seventh International Symposium on Micro Machine and Human Science*, Nagoya, Japan, 2-4 October 1996, pp. 223-228.
- [Cheung, 1997] P Cheung, AA Berlin, DK Biegelisen, WB Jackson, "Batch Fabrication of Pneumatic Valve Arrays by Combining MEMS with Printed Circuit Board Technology," *ASME MEMS 1997*, DSC-vol 62, HTD-vol 354, pp. 39-46.
- [Fearing, 1998] RS Fearing, "Powering 3 Dimensional Micro-robots: Power Density Limitations," *1998 Tutorial on Micro Mechatronics and Micro Robotics*.
- [Goll, 1997] C Goll, W Bacher, B Bustgens, D Maas, R Ruprecht, WK Schomburg, "An Electrostatically Actuated Polymer Microvalve Equipped with a Movable Membrane Electrode," *Journal of Micromechanics and Microengineering*, vol 7, no 3, September 1997, pp. 224-226.
- [Haji-Babaei, 1997] J Haji-Babaei, CY Kwok, RS Huang, "Integrable active microvalve with surface micromachined curled-up actuator," *Transducers '97*, Chicago, IL, 16-19 June 1997, pp. 833-836.
- [Hermida, 1998] A Hermida, "Deflection and Stresses in Circular Membranes Due to Transverse and In-Plane Loading Conditions," NASA Technical Brief GSC-14223.
- [Hoerbiger-Origina] Hoerbiger-Origina, Piezo 2000 product literature, www.hoerbiger-origina.com.
- [Kohl, 1999] M Kohl, KD Skrobaneck, S Miyazaki, "Development of stress-optimized shape memory microvalves," *Sensors and Actuators A (Physical)*, vol. A72, no. 3, February 1999, pp. 243-250.
- [Landis/Staefa] Landis/Staefa, Digital Pneumatic Valve product literature, www.landisstaeafa.com.
- [Lee Company] Lee Company, High Density Interface 3-way solenoid valve product literature, www.theleeco.com.
- [Lisec, 1996] T Lisec, M Kreutzer, B Wagner, "A Bistable Pneumatic Microswitch for Driving Fluidic Components," *Sensors and Actuators A (Physical)*, vol. 54, no. 1-3, June 1996, pp. 746-749.
- [Lucas Novasensor] KR Williams, NI Maluf, EN Fuller, RJ Barron, DP Jaeggi, BP van Driehuisen, "A Silicon Microvalve for the Proportional Control of Fluids," *Transducers '99*.
- [Magnet Sales and Manufacturing] Magnet Sales and Manufacturing Inc., *Magnet Design Guide*, www.magnetsales.com.
- [Meckes, 1997] A Meckes, J Behrens, W Benecke, "Electromagnetically Driven microvalve Fabricated in Silicon," *Transducers 97*, Chicago, IL, 16-19 June 1997, pp. 821-824.
- [Messner, 1998] S Messner, M Muller, V Burger, J Schaible, H Sandmaier, R Zengerle, "A Normally-Closed, Bimetallically actuated 3-Way Microvalve for Pneumatic Applications," *Proceedings MEMS 1998*, pp. 40-44.
- [Monkman, 1988] GJ Monkman, PM Taylor, "Electrostatic Grippers, Principles and Practice," *Proceedings of the International Symposium on Industrial Robots*, April 1988, pp. 193-200.

- [Moy, 2000] G Moy, C Wagner, RS Fearing, "A Compliant Tactile Display for Teletaction," *IEEE International Conference on Robotics and Automation*, April 2000.
- [Ohnstein, 1990] T Ohnstein, T Fukiura, J Ridley, U Bonne, "Micromachined Silicon Microvalve," *Proceedings IEEE Micro Electro Mechanical Systems*, Napa Valley, CA, 11-14 February 1990, pp. 95-98.
- [Redwood Microsystems] Redwood Microsystems, NC-1500 microvalve product literature, www.redwoodmicro.com.
- [Robertson, 1996] JK Robertson, KD Wise, "An Electrostatically-Actuated Microvalve for Semiconductor Gas Flow," *Solid-State Sensor and Actuator Workshop*, Hilton Head, SC, 2-6 June 1996, pp. 148-151.
- [Shearer, 1956] JL Shearer, "Study of Pneumatic Processes in the Continuous Control of Motion with Compressed Air-I," *Transactions of the ASME*, February 1956, pp. 233-242.
- [Timoshenko, 1959] S Timoshenko, S Woinowsky-Krieger, *Theory of Plates and Shells*, New York: McGraw-Hill, 1959.
- [TiNi Alloy] Tini Alloy Company, TiNi microvalve product literature, www.sma-mems.com.
- [Wang, 2000] G Wang, I Kao, "Intelligent Soft Contact Surface Technology with MEMS in Robotic and Human Augmented Systems," *IEEE International Conference on Robotics and Automation*, April 2000.
- [Yang, 1997] X Yang, C Grosjean, YC Tai, CM Ho, "A MEMS Thermopneumatic Silicone Membrane Valve," *Proceedings IEEE Micro Electro Mechanical Systems*, Nagoya, Japan, 26-30 January 1997, pp. 114-118.